Ion-Exosphere with Asymmetric Velocity Distribution

J. LEMAIRE AND M. SCHERER
Belgian Institute for Space Aeronomy, 1180 Brussels, Belgium
(Received 7 September 1971; final manuscript received 11 January 1972)

The number density, the particle flux, the momentum fluxes, and the energy flux are calculated in a model ion exosphere with an open magnetic field, for an asymmetric Maxwellian velocity distribution (i.e., $\sim\exp[-\beta(\mathbf{v}-\mathbf{u})^2]$). Numerical calculations for the polar ionosphere of the earth show that this asymmetry does not qualitatively affect the results obtained with a symmetric velocity distribution function ($u=0$), i.e., the protons are accelerated outward and escape with a supersonic flow speed.

I. INTRODUCTION

Recently, Lemaire and Scherer,[1] determined the number density, the flux, the pressure tensor components, and the energy flux in a simple model ion-exosphere of a nonrotating planet with an open magnetic field. They used the following assumptions: (a) The exosphere is separated from the barosphere or collision-dominated region by a sharply defined surface called the baropause. (b) The magnetic field strength is a monotonic decreasing function along a field line, reaching a minimum at infinity. (c) In the exosphere the particle trajectories can be determined by the well known nonrelativistic guiding center approximation, and the particle drift across magnetic field lines can be neglected. Under these assumptions the exospheric particles can be classified into four conventional classes: (1) the ballistic particles which emerge from the barosphere but cannot escape, (2) the escaping particles which leave the barosphere and are lost in interplanetary space, (3) the trapped particles which have two mirror points in the exosphere between which they bounce continuously up and down, and (4) the incoming particles which originate from the outermost regions.

Assuming a symmetric Maxwellian velocity distribution function at the baropause [i.e., $\sim\exp(-\beta v^2)$], the velocity distribution in the collision-free exosphere was calculated by applying Liouville's theorem. In the special case of a vanishing magnetic field at infinity, Lemaire and Scherer[1,2] applied this model ion exosphere to the polar topside ionosphere of the earth. For an (O^+–H^+-e) exosphere they found that the thermal electrons and oxygen ions are decelerated by the combined effect of the induced electric field and the gravitational field. The protons, however, are accelerated outward and rapidly reach a supersonic flow speed. In this paper the formulas obtained previously will be generalized by assuming that the velocity distribution function of the particles at the baropause is Maxwellian but asymmetric. This seems to be a more realistic model for application to the terrestrial polar ionosphere since it has been found that the effusion velocity of the protons is nearly sonic at the baropause[2] and other recent investigations[3–8] have also shown that a supersonic outward flow of H^+ exists in this region. Numerical calculations, however, show that the mean features obtained with a symmetric Maxwellian distribution function remain. In Sec. II we determine the velocity distribution in the exosphere. In Sec. III we calculate the number density and particle flux, the pressure tensor components and the energy flux; and finally, in Sec. IV we investigate numerically the influence of an asymmetry in the velocity distribution function, for a model ion exosphere of the earth.

For a detailed study of the equations of motion and the classification of the exospheric particles we refer to a previous paper.[1]

II. THE VELOCITY DISTRIBUTION

If the effusion velocity of a constituent is comparable to the thermal speed of this species, the velocity distribution of these particles is highly asymmetric in the direction parallel to the flow. Therefore, we assume that for particles emerging from the barosphere, the actual velocity distribution function at the baropause can be approximated by

$$f(\mathbf{r}_0, \mathbf{v}) = n_0(m/2\pi kT_0)^{3/2}\exp[-(m/2kT_0)(\mathbf{v}-\mathbf{u})^2], \tag{1}$$

where k is the Boltzmann constant, m is the mass of particles, r_0 is the radial distance of the baropause, n_0 and T_0 are constants, and $\mathbf{u}$ represents a velocity vector parallel to the magnetic field $\mathbf{B}(\mathbf{r}_0)$. These parameters are chosen to obtain at the baropause, respectively, a given number density $n(\mathbf{r}_0)$, temperature $T(\mathbf{r}_0)$, and bulk velocity $w(\mathbf{r}_0)$ which is the ratio of the escape flux $F(\mathbf{r}_0)$ to $n(\mathbf{r}_0)$. Since the moments of the velocity distribution are function of the parameters n_0, T_0, and u (see Sec. III), the relation between n_0 and $n(\mathbf{r}_0)$, T_0 and $T(\mathbf{r}_0)$, u and $w(\mathbf{r}_0)$ can be determined.

Even in the case of a symmetric velocity distribution function ($u=0$) the effusion velocity at the baropause is not zero. This is a consequence of the truncation of the velocity distribution to exclude the incoming particles. The actual velocity distribution at the baropause can be quite different from (1) or any linear combination of Maxwellians. It will always

be possible, however, to determine the parameters $n_0, T_0, u, \cdots$; in order to fit a fixed number of moments of the approximated velocity distribution to the corresponding moments of the actual distribution.

The velocity distribution in the exosphere is obtained by solving Vlasov's equation subject to the boundary condition (1)

$$f(\mathbf{r}, \mathbf{v}) = n_0(m/2\pi kT_0)^{3/2} \exp\{-(m/2kT_0)[v^2+R+u^2 - 2u(v^2+R-\eta^{-1}v^2\sin^2\theta)^{1/2}]\}. \quad (2)$$

where R is defined by

$$R=-2\Phi[1+\alpha-(1+\beta)y], \qquad y=r_0/r, \quad (3)$$

$$\alpha=Ze\varphi_0(\mathbf{r}_0)/m\Phi, \qquad \beta=Ze\varphi_0(\mathbf{r})/m\Phi, \quad (4)$$

and where θ is the pitch angle of the particle with mass m, charge Ze, and velocity v; Φ is the gravitational potential at the baropause level, φ_0 is the electrostatic potential due to the small charge separation, and $\eta=B(\mathbf{r})/B(\mathbf{r}_0)$ is the ratio of the magnetic field strength at the radial distance r to the magnetic field strength at the baropause.

III. MOMENTS OF THE VELOCITY DISTRIBUTION

In this section we determine the formulas for the number density, the particle flux parallel to the magnetic field, the parallel and perpendicular momentum fluxes, and the energy flux, for particles with velocity distribution (2). These macroscopic quantities are defined as the different moments of the velocity distribution in a previous paper[1] and we will use the same notations here.

A. Ballistic Particles

It can be shown[1] that the ballistic particles have a positive potential energy $\frac{1}{2}mR$ and that the velocity space corresponding to this class of particles is given by

$$0\le v\le v_b, \qquad 0\le\theta\le\pi, \qquad 0\le\varphi<2\pi;$$

$$v_b\le v\le v_\infty, \quad \begin{cases} 0\le\theta\le\theta_m, \\ \pi-\theta_m\le\theta\le\pi, \end{cases} \quad 0\le\varphi<2\pi; \quad (5)$$

$$v_\infty\le v\le v_c, \quad \begin{cases} \theta_m'\le\theta\le\theta_m, \\ \pi-\theta_m\le\theta\le\pi-\theta_m', \end{cases} \quad 0\le\varphi<2\pi;$$

with

$$v_b^2=\eta R/(1-\eta), \qquad v_\infty^2=-2\Phi(1+\beta)y,$$
$$v_c^2=-2\Phi a(1+\alpha)/(1-a)-2\Phi(1+\beta)y,$$
$$\theta_m=\arcsin[\eta^{1/2}(1+R/v^2)^{1/2}], \quad (6)$$
$$\theta_m'=\arcsin[\mu^{1/2}(1-v_\infty^2/v^2)^{1/2}],$$
$$a=B(\infty)/B(\mathbf{r}_0), \qquad \mu=\eta/a=B(\mathbf{r})/B(\infty).$$

The angle φ is measured in a plane normal to the magnetic field.

Taking into account the explicit form of the velocity distribution function (2) and velocity space (5), it is easy to show that the particle and energy fluxes parallel to the magnetic field are zero. The particle density can be calculated by means of

$$n^{(B)}(\mathbf{r}) = \frac{4}{\pi^{1/2}} n_0 \exp[-(U^2+q)]\Big(\int_0^{V_b} g_1(V)\,dV \times\int_0^{\pi/2} g_2(V,\theta)\,d\theta+\int_{V_b}^{V_\infty} g_1(V)\,dV\int_0^{\theta_m} g_2(V,\theta)\,d\theta + \int_{V_\infty}^{V_c} g_1(V)\,dV\int_{\theta_m'}^{\theta_m} g_2(V,\theta)\,d\theta\Big), \quad (7)$$

in which the following notations are introduced:

$$g_1(V)=V^2\exp(-V^2),$$

$$g_2(V,\theta)=\exp[2U(V^2+q-\eta^{-1}V^2\sin^2\theta)^{1/2}]\sin\theta,$$

$$q=mR/2kT_0, \qquad Z=z(m/2kT_0)^{1/2},$$

where z stands for u, v, v_b, v_∞, and v_c.

In order to reduce the double integrals to simple integrals we use the transformation

$$V=(x^2+y^2-q)^{1/2}, \qquad \theta=\arcsin[\eta^{1/2}x/(x^2+y^2-q)^{1/2}]. \quad (8)$$

which yields the Jacobian

$$\left|\frac{\partial(V,\theta)}{\partial(x,y)}\right| = \eta^{1/2}y(px^2+y^2-q)^{-1/2}(x^2+y^2-q)^{-1/2},$$

with $p=1-\eta$.

Inserting this in (7) gives

$$n^{(B)}(\mathbf{r}) = \frac{4}{\pi^{1/2}} n_0\eta\exp(-U^2)\int_{G_1}\int h(x,y)\,dx\,dy, \quad (9)$$

with

$$h(x,y)=xy(px^2+y^2-q)^{-1/2}\exp[-(x^2+y^2)+2Uy], \quad (10)$$

and where the integration is to be taken over the region G_1, illustrated in Fig. 1.

Performing the x integration we finally obtain

$$n^{(B)}(\mathbf{r})=2n_0\gamma[H(0,A,S_1)-H(q^{1/2},A,T_1)], \quad (11)$$

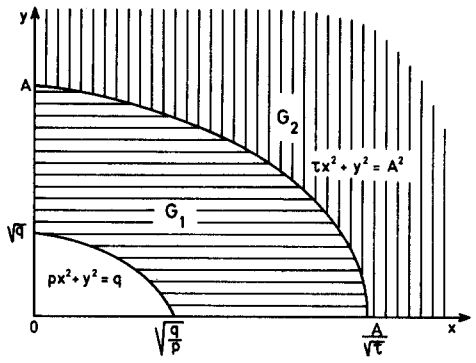

FIG. 1. Domains of integration for the ballistic (G_1) and escaping (G_2) particles.

where, for convenience, we used the shorthand notations

$$H(s,t,S)=\int_s^t S(y)\,y\exp(\eta p^{-1}y^2+2Uy)\,dy,$$
$$S_1=\operatorname{erf}[p^{-1/2}(X^2+a\sigma\tau^{-1}y^2)^{1/2}],$$
$$T_1=\operatorname{erf}[p^{-1/2}(y^2-q)^{1/2}],$$
$$\tau=1-a\geq 0,\qquad \sigma=\mu-1\geq 0, \tag{12}$$
$$A^2=-\Phi m(1+\alpha)/kT_0\geq 0,$$
$$X^2=-\Phi m[(1+\beta)y-a\sigma\tau^{-1}(1+\alpha)]/kT_0,$$
$$\gamma=\eta p^{-1/2}\exp[-(U^2+qp^{-1})];$$

with the error function $\operatorname{erf}(z)$ given by

$$\operatorname{erf}(z)=\frac{2}{\pi^{1/2}}\int_0^z e^{-t^2}\,dt.$$

Formula (11) gives the number density distribution for ballistic particles in the exosphere. The two functions H on the right-hand side of (11) have to be evaluated by numerical integration.

To calculate the momentum fluxes we proceed in a similar way. The region of integration in the xy plane remains G_1 since it is only determined by the velocity space (5). The function $h(x, y)$ in (9), however, is determined by the moment of the velocity distribution. For the parallel and perpendicular momentum fluxes, for example, we have, respectively,

$$h(x,y)=2kT_0xy(px^2+y^2-q)^{1/2}\exp[-(x^2+y^2)+2Uy],$$

and

$$h(x,y)=kT_0\eta x^3y(px^2+y^2-q)^{-1/2}\times\exp[-(x^2+y^2)+2Uy].$$

After some calculations we obtain

(a) The parallel momentum flux

$$P_{||}^{(B)}(\mathbf{r})=4p_0\gamma p[H(0,A,S_2)-H(q^{1/2},A,T_2)], \tag{13}$$

with

$$p_0=n_0kT_0,$$
$$S_2=K_2[p^{-1/2}(x^2+a\sigma\tau^{-1}y^2)^{1/2}],$$
$$T_2=K_2[p^{-1/2}(y^2-q)^{1/2}].$$

The function $K_2(z)$ is defined by

$$K_2(z)=\frac{2}{\pi^{1/2}}\int_0^z t^2e^{-t^2}\,dt,$$

and can be expressed in terms of the error function and the exponential function[1].

(b) The perpendicular momentum flux

$$P_{\perp}^{(B)}(\mathbf{r})=2p_0\gamma\eta[H(0,A,S_3)-H(q^{1/2},A,T_3)], \tag{14}$$

with

$$S_3=S_2-p^{-1}(y^2-q)S_1,\qquad T_3=T_2-p^{-1}(y^2-q)T_1.$$

B. Escaping Particles

For this class of particles we have to make a difference between particles with a positive and a negative potential energy $\frac{1}{2}mR$. Lemaire and Scherer[1] have shown that in the former case the velocities v and the pitch angles θ are limited by the following inequalities

$$v_\infty\leq v\leq v_c,\qquad 0\leq\theta\leq\theta_m';$$
$$v_c\leq v<\infty,\qquad 0\leq\theta\leq\theta_m;$$

so that the particle density can be calculated by means of

$$n^{(E)}(\mathbf{r})=\frac{2}{\pi^{1/2}}n_0\exp[-(U^2+q)]\left(\int_{V_\infty}^{V_c}g_1(V)\,dV\times\int_0^{\theta_m'}g_2(V,\theta)\,d\theta+\int_{V_c}^{\infty}g_1(V)\,dV\int_0^{\theta_m}g_2(V,\theta)\,d\theta\right). \tag{15}$$

Taking into account transformation (8), expression (15) can be reduced to

$$n^{(E)}(\mathbf{r})=\frac{2}{\pi^{1/2}}n_0\eta\exp(-U^2)\int_{G_2}\int h(x,y)\,dx\,dy, \tag{16}$$

where the region of integration G_2 is shown in Fig. 1, and the integrand $h(x, y)$ is defined in (10).

The double integral on the right-hand side of (16) can be reduced to two simple integrals which yields

$$n^{(E)}(\mathbf{r})=n_0\gamma[H(0,A,S_4)+H(A,\infty,T_4)], \tag{17}$$

with

$$S_4=1-S_1,\qquad T_4=1-T_1.$$

Similar calculations give:

(a) The parallel momentum flux

$$P_{||}^{(E)}(\mathbf{r})=2p_0\gamma p[H(0,A,S_5)+H(A,\infty,T_5)], \tag{18}$$

with

$$S_5=0.5-S_2, \qquad T_5=0.5-T_2.$$

(b) The perpendicular momentum flux

$$P_\perp^{(E)}(\mathbf{r})=p_0\gamma\eta[H(0, A, S_6)+H(A, \infty, T_6)], \quad (19)$$

with

$$S_6=S_5-p^{-1}(y^2-q)S_4, \qquad T_6=T_5-p^{-1}(y^2-q)T_4.$$

To determine the particle and energy fluxes we can still use the transformation (8) where the integration over the region G_2 can now be performed analytically. The corresponding moments of the velocity distribution, however, can also be calculated straightforward. For the particle flux this yields

$$F^{(E)}(\mathbf{r})=\tfrac{1}{4}n_0c\eta(W+X-Y+Z), \quad (20)$$

with

$$c=(8kT_0/\pi m)^{1/2}, \qquad W=a^{-1}\exp[-(A-U)^2],$$
$$X=\pi^{1/2}U\,\mathrm{erfc}(A-U), \quad (21)$$
$$Y=a^{-1}\tau\exp[-(\tau^{-1}A^2+U^2)],$$
$$Z=\pi^{1/2}U(\tau/a)^{3/2}[\mathfrak{D}(a^{-1/2}\tau^{1/2}U)-\mathfrak{D}(a^{1/2}\tau^{-1/2}A+a^{-1/2}\tau^{1/2}U)]\exp[-(\tau^{-1}A^2+a^{-1}U^2)].$$

The complementary error function and Dawson's integral are, respectively, defined by

$$\mathrm{erfc}(z)=\frac{2}{\pi^{1/2}}\int_z^\infty \exp(-t^2)\,dt=1-\mathrm{erf}(z),$$

and

$$\mathfrak{D}(z)=\frac{2}{\pi^{1/2}}\int_0^z \exp(t^2)\,dt.$$

On the other hand, we can calculate the energy flux by means of

$$\epsilon(\mathbf{r})=\tfrac{1}{4}p_0c\eta\{[2-q+(1-a^{-1}\tau)U^2+UA+A^2]\times W+(U^2-q+2.5)X-PY+(P+0.5)Z\}, \quad (22)$$

where

$$P=2-q-a^{-1}\tau U^2+\tau^{-1}A^2.$$

For escaping particles with a negative potential energy it was shown[1] that the velocity space is determined by

$$(-R)^{1/2}\leq v<\infty, \qquad 0\leq\theta\leq\theta_m, \qquad 0\leq\varphi<2\pi.$$

Applying transformation (8), the particle density is given by

$$n^{(E)}(\mathbf{r})=\frac{2}{\pi^{1/2}}n_0\eta\exp(-U^2)\int_0^\infty dy\int_0^\infty h(x, y)\,dx, \quad (23)$$

where $h(x, y)$ is defined in (10).

TABLE I. Effusion velocity (w_{H^+}) and escape flux (F_{H^+}) at the baropause for different degrees of asymmetry (u_{H^+}) in the proton velocity distribution.

u_{H^+} km sec^{-1}	u_{H^+}/c_{H^+}	$w_{H^+}(r_0)$ km sec^{-1}	$w_{H^+}(r_0)/c_{H^+}$	$F_{H^+}(r_0)$ cm^{-2} sec^{-1}
0	0	4.0	0.5	4.0×10^7
5	0.6	6.3	0.8	6.3×10^7
10	1.2	10.3	1.3	1.0×10^8

The right-hand side of (23) is a special case ($A=0$) of the double integral in (16). By making the formal substitution $A=0$, we can immediately derive the formulas which give the macroscopic quantities for particles with a negative potential energy, from the corresponding expressions derived for the escaping particles with a positive potential energy.

IV. NUMERICAL RESULTS

It is easy to check that for $u\to0$, the formulas deduced in Sec. III, reduce to the corresponding expressions, given by Lemaire and Scherer.[1] To exhibit the influence of an asymmetry in the velocity distribution of the particles in the terrestrial polar ion exosphere we consider an (O^+–H^+–e)-exosphere with a vanishing magnetic field at infinity. Moreover, we use a dipole configuration for the terrestrial magnetic field up to a radial distance of about four earth radii. The baropause is chosen at 2000 km above the polar cap, the ion and electron temperatures at this level are 3000°K, and the concentrations are $n_e(r_0)=10^3$ cm^{-3}, $n_{O^+}(r_0)=9\times10^2$ cm^{-3}, and $n_{H^+}(r_0)=10^2$ cm^{-3}.

Furthermore, we take a symmetric Maxwellian velocity distribution for the oxygen ions ($u_{O^+}=0$) since their effusion velocity is very small compared with the O^+ mean thermal speed [$w_{O^+}(r_0)/c_{O^+}\simeq10^{-9}$]. The effect of an asymmetry in the electron velocity distribution (corresponding to parameter values $u_e\leq10$ km sec^{-1}) is also negligible [$w_e(r_0)/c_e\simeq10^{-3}$]. Therefore, we confine ourselves to the study of the influence of an asymmetric proton velocity distribution.

In what follows we considered three values of the parameter u_{H^+}, i.e., 0, 5, and 10 km sec^{-1}. We computed the macroscopic quantities calculated in Sec. III along a magnetic field line which intersects the baropause at a geomagnetic latitude of 80°. The results do not differ significantly with the choice of the open field line. Moreover, we neglect the incoming particles, and assume that the trapped electrons and oxygen ions are in thermal equilibrium, respectively, with the electrons and O^+ emerging from the barosphere. The number density and momentum fluxes for these trapped particles were determined in a previous paper,[1] to which we also refer for a detailed description of the method of computation.

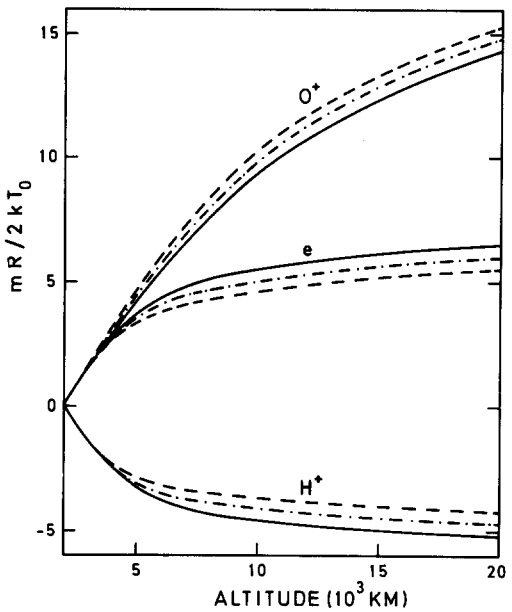

FIG. 2. Reduced potential energies versus altitude along a magnetic field line crossing the baropause (2000-km altitude) at 80° latitude. At the baropause each species has a temperature of 3000°K, and the concentrations are $n_e=10^3$ cm^{-3}, $n_{O^+}=9\times10^2$ cm^{-3}, and $n_{H^+}=10^2$ cm^{-3}. The solid, the dot-dashed, and the dashed lines, respectively, correspond to the values of the parameter $u_{H^+}=0$, 5, and 10 km sec^{-1}.

Table I gives the value of the effusion velocity or bulk velocity $w_{H^+}(\mathbf{r}_0)$ and the escape flux $F_{H^+}(\mathbf{r}_0)$ of the hydrogen ions at the baropause. The bulk velocity is always larger than u_{H^+}. Only for unreasonably high asymmetric velocity distribution functions, does $w_{H^+}(\mathbf{r}_0)$ become nearly equal to u_{H^+}. The escape flux of the protons increases with u_{H^+} since in the three models we assumed the same concentrations at the baropause level.

The reduced potential energy $mR/2kT_0$ is plotted for each species in Fig. 2, which shows that for growing values of the parameter u_{H^+}, the total potential energy $\frac{1}{2}mR$ increases for the ions but decreases for the electrons. Qualitatively, however, there is no difference from the results obtained with a symmetric proton velocity distribution (represented by a solid line). The electrons and oxygen ions have a monotonic

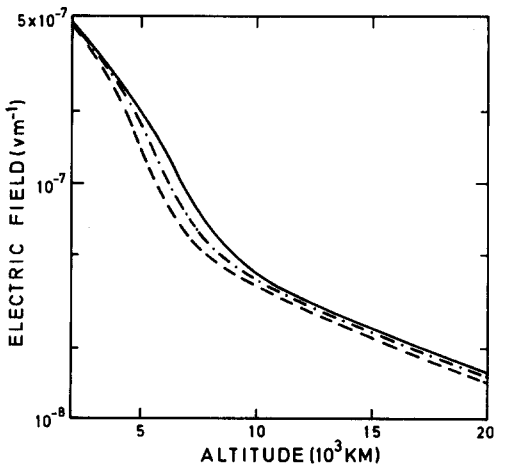

FIG. 3. The electric field distribution along a magnetic field line crossing the baropause (2000-km altitude) at 80° latitude. At the baropause the ion and electron temperatures are 3000°K, and the concentrations are $n_e=10^3$ cm^{-3}, $n_{O^+}=9\times10^2$ cm^{-3}, and $n_{H^+}=10^2$ cm^{-3}. The solid, the dot-dashed, and the dashed line, respectively, correspond to the values of $u_{H^+}=0$, 5, and 10 km sec^{-1}.

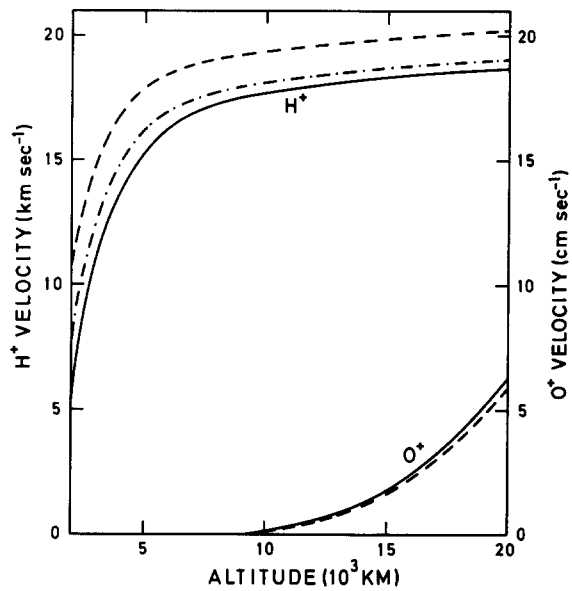

FIG. 4. The bulk velocity versus altitude along a magnetic field line crossing the baropause (2000-km altitude) at 80° latitude. At the baropause the ion and electron temperatures are 3000°K, and the concentrations are $n_e=10^3$ cm^{-3}, $n_{O^+}=9\times10^2$ cm^{-3}, and $n_{H^+}=10^2$ cm^{-3}. The solid, the dot-dashed, and the dashed lines, respectively, correspond to the values of $u_{H^+}=0$, 5 and 10 km sec^{-1}.

increasing positive potential energy distribution and therefore are decelerated. The protons on the contrary are blown out since they have a monotonic decreasing negative potential energy. The escape flux of the thermal electrons is determined by the electric potential difference between the baropause and infinity. Moreover, the electron flux will be equal to the proton flux because the escape of oxygen ions is negligible. Since the proton flux, increases with u_{H^+}, the electron escape flux will also increase and, therefore, the potential barrier, which the escaping electrons have to overcome, must decrease.

Figure 3 illustrates how the electric field intensity in the exosphere diminishes with increasing u_{H^+}. As a consequence the acceleration of the ions is also reduced. Therefore, although the effusion velocity at

the baropause increases significantly with u_{H^+}, the bulk velocity at high altitudes is not much different from the constant value corresponding to a symmetric velocity distribution function. This is shown in Fig. 4 where we plotted the bulk velocity of the protons in km sec^{-1} (left-hand scale) and of the oxygen ions in cm sec^{-1} (right-hand scale).

The ion number densities versus altitude are given in Fig. 5. Note that although n_{H^+} increases and n_{O^+} decreases for an increasing asymmetry in the velocity distribution function, the scale height is practically not affected above 6000 km in altitude.

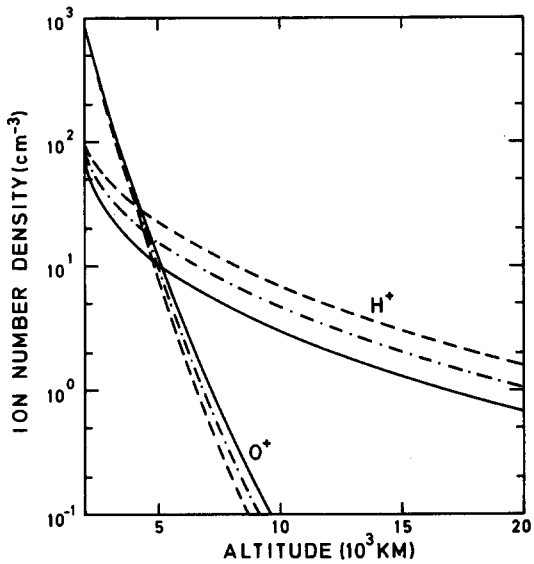

FIG. 5. The ion number densities versus altitude along a magnetic field line crossing the baropause (2000-km altitude) at 80° latitude. At the baropause each species has a temperature of 3000°K, and the concentrations are $n_e=10^3$ cm^{-3}, $n_{O^+}=9\times10^2$ cm^{-3}, and $n_{H^+}=10^2$ cm^{-3}. The solid, the dot-dashed, and the dashed lines, respectively, correspond to the values of $u_{H^+}=0$, 5, and 10 km sec^{-1}.

In Fig. 6 we illustrate the average temperature and the temperature anisotropy distributions. For the oxygen ions the temperature is nearly independent of u_{H^+} and remains practically constant and isotropic. The electron temperature decreases slightly and the growth of the anisotropy is very small for an increasing asymmetry of the proton velocity distribution. The effect upon the hydrogen average temperature and temperature anisotropy, however, is much more pronounced; both become larger with increasing values of u_{H^+}.

Finally, we give the proton and electron conduction flux versus altitude in Fig. 7, which shows growth with an increasing degree of asymmetry for both constituents. The electron conduction flux is approximately two orders of magnitude larger than the con-

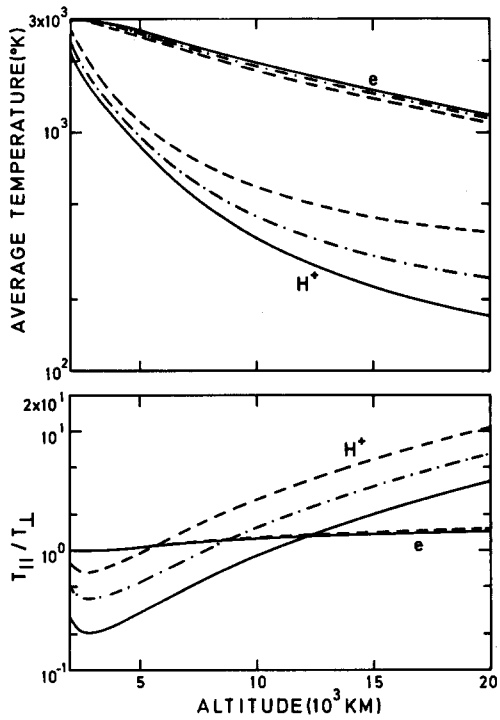

FIG. 6. The average temperatures and temperature anisotropies versus altitude along a magnetic field line crossing the baropause (2000-km altitude) at 80° latitude. At the baropause each species has a temperature of 3000°K, and the concentrations are $n_e=10^3$ cm^{-3}, $n_{O^+}=9\times10^2$ cm^{-3}, and $n_{H^+}=10^2$ cm^{-3}. The solid, the dot-dashed, and the dashed lines, respectively, correspond to the values of $u_{H^+}=0$, 5 and 10 km sec^{-1}.

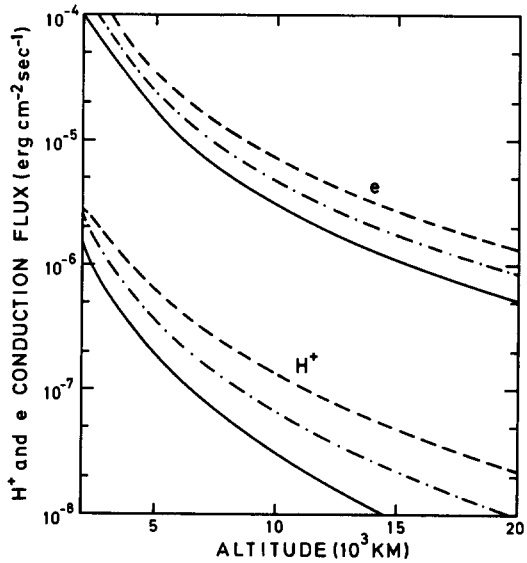

FIG. 7. The conduction flux distributions along a magnetic field line crossing the baropause (2000-km altitude) at 80° latitude. At the baropause the ion and electron temperatures are 3000°K, and the concentrations are $n_e=10^3$ cm^{-3}, $n_{O^+}=9\times10^2$ cm^{-3}, and $n_{H^+}=10^2$ cm^{-3}. The solid, the dot-dashed, and the dashed lines, respectively, correspond to the values of $u_{H^+}=0$, 5 and 10 km sec^{-1}.

duction flux of the ions, which is practically equal to the proton conduction flux.

V. CONCLUSIONS

Although a reasonable value of the parameter u_{H^+} will probably not exceed a small fraction of the thermal speed, we considered the influence of very large asymmetries in the velocity distribution function at the baropause. The results presented above, show that for the terrestrial polar ion exosphere, the most salient properties are qualitatively not affected by considering such an asymmetry, i.e.:

(1) The protons are accelerated outward by a small electric field which retains the electrons.

(2) The proton flow speed rapidly becomes supersonic, but the oxygen ions are bound to the earth by the gravitational force which is larger than the electric force.

ACKNOWLEDGMENT

We appreciate the valuable advice and continuous interest of Professor Dr. M. Nicolet during the preparation of this work.

[1] J. Lemaire and M. Scherer, Phys. Fluids **14**, 1683 (1971).
[2] J. Lemaire and M. Scherer, Planet. Space Sci. **18**, 103 (1970).
[3] P. M. Banks and T. E. Holzer, J. Geophys. Res. **73**, 6846 (1968).
[4] P. M. Banks and T. E. Holzer, J. Geophys. Res. **74**, 6317 (1969).
[5] J. H. Hoffman, Intern. J. Mass. Spectry. Ion Phys. **4**, 315 (1970).
[6] K. Marubashi, J. Radiation Res. Lab. **17**, 335 (1970).
[7] K. Marubashi, Rept. Ionospheric Space Res. (Japan) **24**, 323 (1970).
[8] T. E. Holzer, J. A. Fedder, and P. M. Banks, J. Geophys Res. **76**, 2453 (1971).

THE PHYSICS OF FLUIDS VOLUME 15, NUMBER 5 MAY 1972

Numerical Analysis on Source Expansion Flow into Vacuum

TAKEO SOGA* AND HAKURO OGUCHI
Institute of Space and Aeronautical Science, University of Tokyo, Tokyo, Japan
(Received 11 June 1971; final manuscript received 23 November 1971)

A numerical analysis of the source expansion flow into a vacuum is presented. Applying the BGK kinetic equation described in spherical coordinates to the problem, it is solved by combining a proposed computational technique with a discrete ordinate method. The actual computation is carried out for a large variety of rarefaction conditions, covering a wide extent from an equilibrium region near the sonic radius up to one sufficiently far downstream. Calculated results for the radial and perpendicular temperatures are compared with results obtained by existing methods.

I. INTRODUCTION

The steady expansion of a gas into a vacuum contains a very important feature of the transition from continuum to free molecule, along with possible applications related to the high intensity molecular beam, rocket exhaust, and so on. In the present paper, we are concerned with the theoretical aspects of this rarefied gas dynamic problem.

Brook and Oman[1] made an analysis by the moment method based on the BGK kinetic equation. As pointed out in Refs. 2 and 3, however some significant terms on the left-hand side of the equation were ignored, so that their results are unlikely to be of more than qualitative value. Edwards and Cheng[2] studied the hypersonic region far downstream from the source, by the moment method based on the BGK kinetic equation, retaining the terms omitted in Ref. 1. At nearly the same time, Hamel and Willis[3] analyzed the whole flow field from the source to the hypersonic region, using the moment equations based on the Boltzmann equation with a hypersonic approximation. An analysis similar to that by Hamel and Willis was recently made by Chen[4] by preserving more higher moments, but it led to results considerably different from those of Hamel and Willis.

The moment method appears to have an uncertainty in the resulting solution, due to the nonuniqueness relevant to the truncation of higher moments. Since, however, the full Boltzmann equation is difficult to solve, it will be treated using the BGK kinetic model. The purpose of this paper is to seek a straightforward solution of the BGK kinetic equation for the problem with far fewer approximations than previous treatments.

II. FORMULATION OF THE PROBLEM

Owing to geometrical symmetry, the BGK kinetic equation in spherical coordinates (r, θ, φ) reduces to

$$V_r \frac{\partial f}{\partial r} + \frac{V_\theta^2 + V_\varphi^2}{r} \frac{\partial f}{\partial V_r} - \frac{V_r V_\theta}{r} \frac{\partial f}{\partial V_\theta} - \frac{V_r V_\varphi}{r} \frac{\partial f}{\partial V_\varphi} = \nu(F - f). \quad (1)$$